Transient Thermal 2D FEM Analysis of SiC Mosfet in Short-Circuit Operation Including Solidus-Liquidus Phase Transition of the Aluminum Source Electrode

Emmanuel Sarraute, Thibauld Cazimajou, Frédéric Richardeau

▶ **To cite this version:**

Emmanuel Sarraute, Thibauld Cazimajou, Frédéric Richardeau. Transient Thermal 2D FEM Analysis of SiC Mosfet in Short-Circuit Operation Including Solidus-Liquidus Phase Transition of the Aluminum Source Electrode. 24th International Conference on Thermal, Mechanical and Multi-Physics Simulation and Experiments in Microelectronics and Microsystems (EuroSimE 2023) - IEEE Electronics Packaging Society, Apr 2023, Graz, Austria. 10.1109/EuroSimE56861.2023.10100775 . hal-04074503

HAL Id: hal-04074503
https://hal.science/hal-04074503

Submitted on 19 Apr 2023

HAL is a multi-disciplinary open access archive for the deposit and dissemination of scientific research documents, whether they are published or not. The documents may come from teaching and research institutions in France or abroad, or from public or private research centers.

L'archive ouverte pluridisciplinaire **HAL**, est destinée au dépôt et à la diffusion de documents scientifiques de niveau recherche, publiés ou non, émanant des établissements d'enseignement et de recherche français ou étrangers, des laboratoires publics ou privés.

Transient Thermal 2D FEM Analysis of SiC Mosfet in Short-Circuit Operation Including Solidus-Liquidus Phase Transition of the Aluminum Source Electrode

Emmanuel Sarraute, Thibauld Cazimajou and Frédéric Richardeau

LAPLACE, Université de Toulouse, CNRS, INPT, UPS, Toulouse, France
emmanuel.sarraute@laplace.univ-tlse.fr

Abstract

Understanding electrothermal SiC power Mosfet behavior in extremely abnormal operations such as short-circuit is a major need for certification, especially for critical or long-life applications. But simulating short-circuits in electronic components is very difficult because we need a fully electric and thermal Multiphysics model. We also need to model the top aluminum electrode melting. We have used the "apparent heat capacity" method to model this melting, which considers the latent heat and the needed absorbed energy during the fusion. So, for the first time, this article presents a numerical finite element model that fully simulates in 2D the dynamic electrothermal behavior of a SiC power transistor in short-circuit regime. The geometric precision of this model provides significant added values compared to existing 1D models.

1. Introduction

SiC Mosfet power device [1] is essential nowadays to gain high efficiency and compactness on medium and high-power converters, for example, inverters in electric vehicles [2]. However, limits of use in extreme accidental conditions such as short-circuit are not fully known with precision [3]: the effective time capability in short-circuit operation, as well as the critical absorption energy of the chip, are essential to calibrate the maximum gate-driver protection delay time to avoid damage, aging and a possible failure of the chip. In addition to reliable dimensioning, the internal management of the electrical safety of a converter has become an essential step in the certification process.

In this article, the authors focus on the modeling, the analysis, and the "time–energy" characterization of the aluminum source electrode melting that appears at the top of the chip in short-circuit operation if the gate-driver protection is insufficient fast. Due to the proximity with the active channel region, possible melting of the source electrode in the event of a short-circuit can induce uncontrolled short-paths through $Si0_2$ cracks between the Al-Ti source layer and the polysilicon gate electrode leading to a V_{GS} chaotic drop voltage as previously illustrated by authors in [4]. Such a scenario is one of the specific limitations of the SiC chip robustness under repetitive short-circuit occurrences, but it is not completely known.

In the recent results obtained by the authors [11], Figure 1 clearly shows melting and evaporation zones with bubbles at the Al-SiC interface and in the bulk of the Al metallization. This result proves that it is insufficient to model only the temperature of the semiconductor active part of the chip SiC. The Al source electrode's phase change solidus–liquidus modeling must be considered to accurately estimate the real temperature transient 2D mapping around the gate electrode, delay times, and energy needed. For future works, this model seems essential to study the thermomechanical aspects of deformation, stress, and cracking of the whole gate region.

This topic has not really been exhaustively studied in the international literature. The authors started to work on modeling the solidus-liquidus phase transition during F. Boige's thesis [4]. A first implementation regarding a SiC Mosfet was successfully carried out in the Comsol Multiphysics software but only in a 1D approach [5]. In [6], an analysis of the influence of several parameters was proposed using a thermal simulation of a SiC MOSFET under short-circuit conditions. More recently, an interesting and precise study of the solid-liquid transition functions to model the thermal phase change behavior of the Al source electrode has been carried out under Ansys software but also remains in 1D [7]. Very recently [8], these same transition laws were applied in 2D but assumed a simplified homogeneous distribution of the heat flow over the entire width of a SiC Mosfet cell to predict the maximum SiC Mosfet junction temperature near the electric field peak value. Such an assumption has also been suggested and widely used by the Toyota R&D center, of which a very interesting insight is described in detail in [9] using Abaqus software.

Emmanuel Sarraute, Thibauld Cazimajou, Frédéric Richardeau, LAPLACE, Université de Toulouse, CNRS, INPT, UPS, Toulouse, France. Postprint Accepted Author Manuscript : https://hal.science/#
24th International Conference on Thermal, Mechanical and Multi-Physics Simulation and Experiments in Microelectronics and Microsystems – IEEE Electronics Packaging Society.
Graz, Austria, April 16 - 19, 2023, Oral Session.

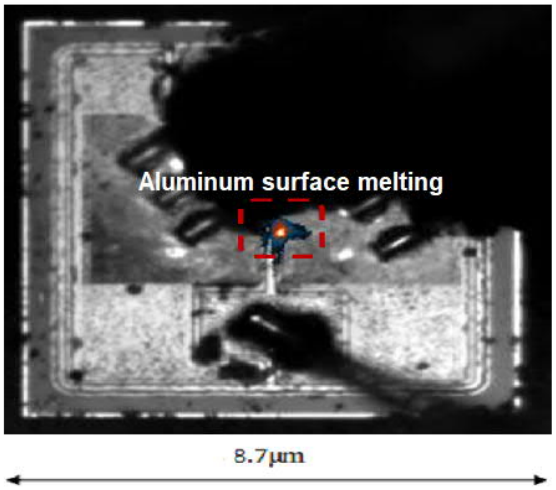

Figure 1a) Top view and cross-section of the planar-gate 1.2kV-80mΩ SiC Mosfet used in this study.

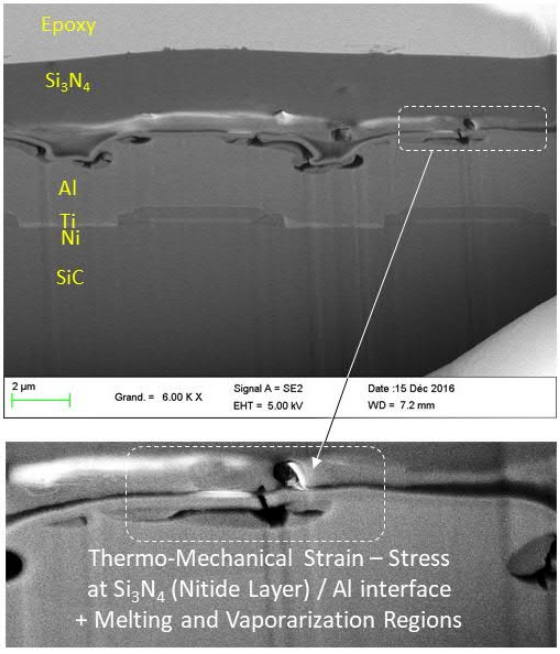

Figure 1b) Pictures of the Al melting and vaporization regions localized at the Al-SiC source interface and in the thick Al electrode after a long-pulse short-circuit operation of the same planar-gate 1.2kV-80mΩ device [11].

In this paper, a new transient "true 2D" Al melting modeling is implemented and used to physically predict the high-temperature solid-liquid phase transition of the source electrode of a SiC Mosfet to be able to determine with good geometric and temporal accuracy, the critical "time-energy" values during the short-circuit. The thermal modeling proposed in this article is based on a prior transient electrothermal 2D model of a SiC Mosfet in short-circuit operation, recently developed by the authors in the same Comsol software. However, this prior electrothermal modeling based on the semiconductor laws of SiC is not explained in this article which is dedicated to considering the phase change of the aluminum source electrode. This paper is organized as follows: in section 2, we describe the theoretical bases of the phase transition model that we used; in section 3, we present the studied SiC Mosfet device and its implementation in the Comsol Multiphysics software; in section 4, the outstanding results are presented and discussed; and finally, in section 5, as a conclusion, an analysis of context and applications is made to show the interest of our 2D approach if one wishes to precisely evaluate the time and energy constraints during a short-circuit.

2. Theoretical bases of aluminum phase change

Let's start with a solid material and trace its enthalpy evolution as a temperature function. Figure 2 shows that a large amount of thermal energy is absorbed at a certain temperature, called melting temperature (when the material changes from a solid to a liquid state). This absorbed thermal energy is called the enthalpy of change of state or latent heat.

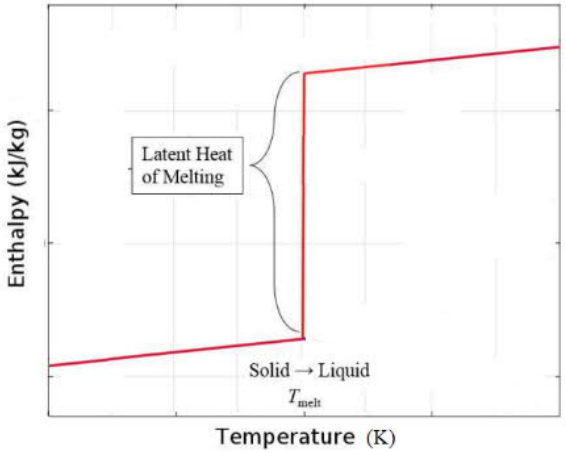

Figure 2 Enthalpy vs. temperature curve and corresponding latent heat of melting.

As we pointed out, this transient phenomenon is very important and must be considered in our electrothermal modeling because it is similar to a theoretically perfect but energy-limited heat sink phenomenon. The method we used is that of the apparent heat capacity [12,13,14].

Emmanuel Sarraute, Thibauld Cazimajou, Frédéric Richardeau, LAPLACE, Université de Toulouse, CNRS, INPT, UPS, Toulouse, France. Postprint Accepted Author Manuscript : https://hal.science/#
24th International Conference on Thermal, Mechanical and Multi-Physics Simulation and Experiments in Microelectronics and Microsystems – IEEE Electronics Packaging Society.
Graz, Austria, April 16 - 19, 2023, Oral Session.

This method considers the enthalpy of state change by integrating it into the heat capacity formulation. If the material is incompressible, the enthalpy depends only on the temperature, and the heat capacity is calculated from the derivative of the enthalpy with respect to the temperature. For reasons of numerical convergence, we understand that it is preferable to impose a gradual phase change over a small finite temperature interval ΔT.

The heat equation to be solved is:

$$\rho(T)C_p(T)\frac{\partial T}{\partial t} = -k(T)\Delta T + P \qquad (1)$$

With :
$\rho(T)$ the density $[kg.m^{-3}]$,
$C_p(T)$ the heat capacity $[J.kg^{-1}.K^{-1}]$,
T the temperature $[K]$,
t le time $[s]$,
$k(T)$ the thermal conductivity $[W.m^{-1}K^{-1}]$,
Δ the Laplace operator,
P the internal heat source $[W.m^{-3}]$.

To consider the smoothed evolution of the enthalpy, we define a change of state parameter $\alpha(T)$ which follows the error function law in the following form:

$$\alpha(T) = \frac{1}{2}\left(1 + erf\left(\frac{T-T_f}{\sigma\sqrt{2}}\right)\right) \qquad (2)$$

With:
T_f the mean,
σ the standard deviation or variance.

And:

$$erf(x) = \frac{2}{\sqrt{\pi}}\int_0^x e^{-t^2}\,dt \qquad (3)$$

The adjustment of the variance allows fixing the temperature interval $\Delta T = 30K$ and the mean allows to impose the melting temperature $T_f = 933K$. Figure 3 shows the evolution of the phase change parameter for aluminum:

The apparent heat capacity is then defined as a function of α(T) as follows:

$$C_p(T) = C_{ps}\big(1-\alpha(T)\big) + C_{pl}\alpha(T) + H_f\frac{d\alpha(T)}{dT} \qquad (4)$$

With:
C_{ps} the solid phase heat capacity $[J.kg^{-1}.K^{-1}]$,
C_{pl} the liquid phase heat capacity $[J.kg^{-1}.K^{-1}]$,
H_f the enthalpy of change of state $[J.kg^{-1}]$.

We check in Figure 4 that the apparent heat capacity follows a Gaussian-type law around the melting temperature and considers the enthalpy of change of state.

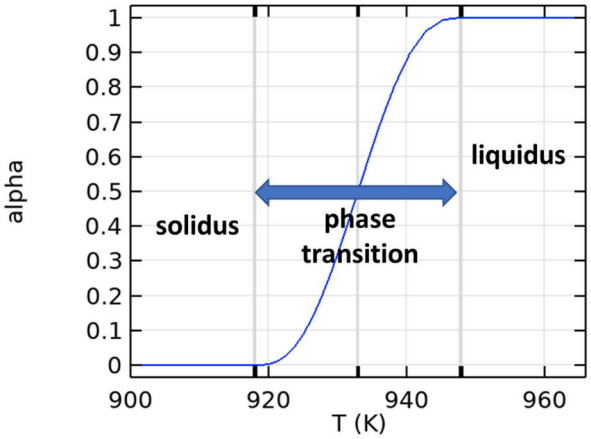

Figure 3 Aluminum transition factor α(T) vs. temperature curve.

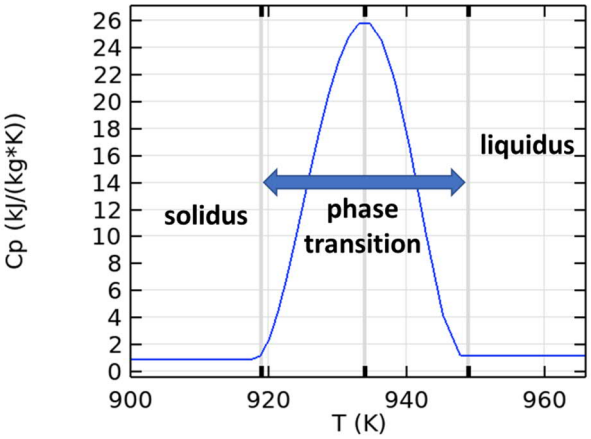

Figure 4 Aluminum heat capacity vs. temperature curve.

As we said previously, because the enthalpy depends only on the temperature and the heat capacity is calculated from the derivative of the enthalpy with respect to the temperature, Figure 5 clearly shows that the resulting enthalpy evolves gradually and that the transition takes place over the temperature range ΔT.

As can be seen in figures 6 and 7, changes in apparent thermal conductivity and apparent density as a function of temperature are considered in the same way:

$$k(T) = k_s\big(1-\alpha(T)\big) + k_l\alpha(T) \qquad (5)$$

$$\rho(T) = \rho_s\big(1-\alpha(T)\big) + \rho_l\alpha(T) \qquad (6)$$

With:
k_s the solid phase thermal conductivity $[W.m^{-1}K^{-1}]$,
k_l the liquid phase thermal conductivity $[W.m^{-1}K^{-1}]$,
ρ_s the solid phase density $[kg.m^{-3}]$,
ρ_l the liquid phase density $[kg.m^{-3}]$.

Emmanuel Sarraute, Thibauld Cazimajou, Frédéric Richardeau, LAPLACE, Université de Toulouse, CNRS, INPT, UPS, Toulouse, France. Postprint Accepted Author Manuscript : https://hal.science/#
24th International Conference on Thermal, Mechanical and Multi-Physics Simulation and Experiments in Microelectronics and Microsystems – IEEE Electronics Packaging Society.
Graz, Austria, April 16 - 19, 2023, Oral Session.

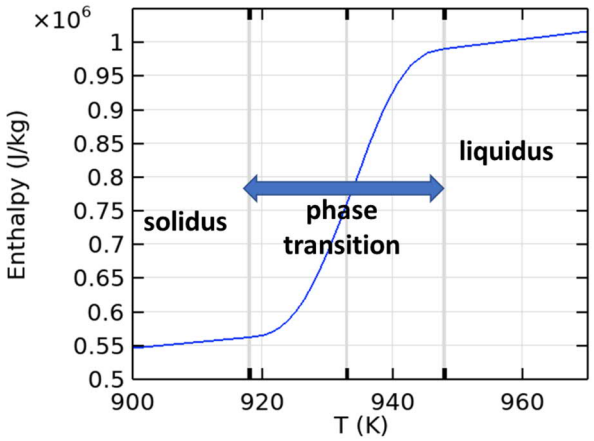

Figure 5 Aluminum smoothed enthalpy vs. temperature curve.

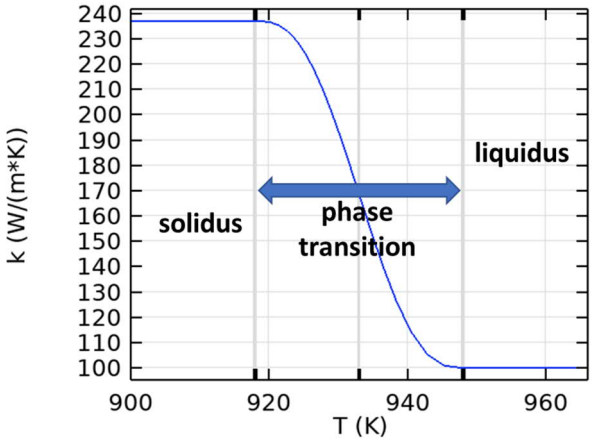

Figure 6 Aluminum thermal conductivity vs. temperature curve.

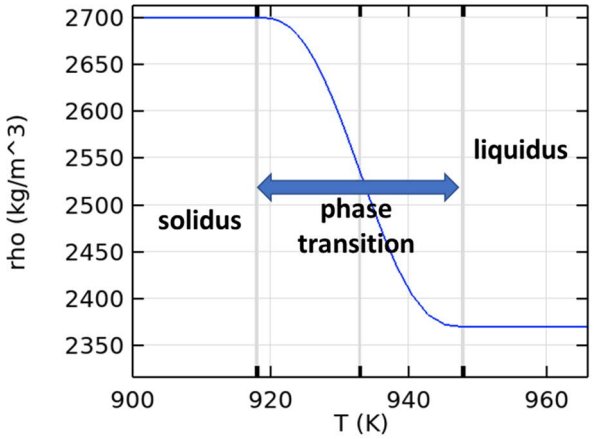

Figure 7 Aluminum density vs. temperature curve.

Table 1 below summarizes the parameters' values related to the aluminum's phase change. Note that all the other materials of our component are not affected by a phase change because their melting temperatures are higher than the temperatures reached.

Tab 1 : Phase-change aluminum parameters

Transition temperature - Tf	933	K
Transition interval - ΔT	30	K
Phase-change enthalpy - Hf	397	$kJ.kg^{-1}$
Solid heat capacity - Cps	900	$J.kg^{-1}.K^{-1}$
Liquid heat capacity - Cpl	1175	$J.kg^{-1}.K^{-1}$
Solid thermal conductivity - ks	237	$W.m^{-1}.K^{-1}$
Liquid thermal conductivity - kl	100	$W.m^{-1}.K^{-1}$
Solid density - ρs	2700	$kg.m^{-3}$
Liquid density - ρl	2370	$kg.m^{-3}$

3. Studied device and 2D model implementation

In this part, we briefly describe the construction of the 2D electrothermal model of our Mosfet (section 1). The principle diagram and the important dimensions are presented in figure 8. In practice, this Mosfet is part of an array of identical active cells in parallel, and we can use geometric, electrical, and thermal symmetries to reduce the numerical model to half a cell.

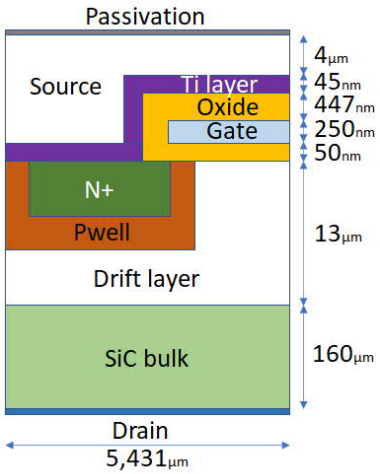

Figure 8 Reduced geometry of the studied model.

Regarding electrical aspects, the drain and source electrodes are biased at 600V and 0V respectively. To turn on the transistor's channel and simulate a short-circuit, we apply a gate voltage Vgs of 20V throughout 5µs.

On a thermal aspect, only the drain electrode boundary is maintained at a constant temperature of 300K imposed by the sole of the component, which acts as a cold source. On the other boundaries, no heat exchange is considered for symmetry or insulation reasons. The upper layer of SiN_3 epoxy passivation as well as the soft solder of the drain-side electrode are not considered because the time horizon of the study (5µs) is very lower than the total diffusion time of the heat through the full thickness of the cell (>100µs).

The precise geometry of the component has been reproduced from a SEM picture of a micro-section of a gen 2 1.2kV-80mΩ SiC Mosfet [4]. Figure 9 shows the real picture of the transistor and the corresponding modeled geometry.

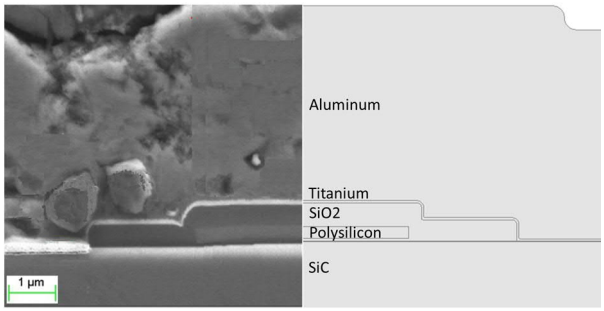

Figure 9 Real picture of the transistor and the corresponding modeled geometry.

The main electrothermal parameters of the materials are given in table 2. It is recalled that even if the electrical losses at the origin of the temperature rise of the component occur in the semiconductor, we do not detail in this article the electrical properties of SiC and the electrical model of the semiconductor. This will be the subject of a future specific publication on the subject.

Tab 2 : Thermal properties of materials

Materials	Density	Thermal Conductivity	Specific Heat
	kg/m³	W/(m.K)	J/(kg.K)
Aluminum solidus	2700	237	900
Aluminum liquidus	2370	100	1175
Titanium	4506	21,9	522
SiO_2	2200	1,4	730
Polysilicon	2320	34	678
4H SiC	2329	131	700

The complete simulation of the short-circuit requires simultaneously solving the electrical equations in the SiC and the thermal ones in the whole model as a function of time. Indeed, the semiconductor properties of SiC and its channel mobility depend very strongly on the local temperature. Finally, as we explained in section 2, we considered the solid-liquid phase change of aluminum.

We have therefore solved, for the first time in 2D, the dynamic electrothermal behavior of a SiC Mosfet in an extreme short-circuit regime by considering the solid-liquid phase change of the aluminum source electrode.

4. Simulation results and discussion

Figures 10 and 11 respectively show the gate voltage and the resulting drain current density chronograms with and without considering the phase change.

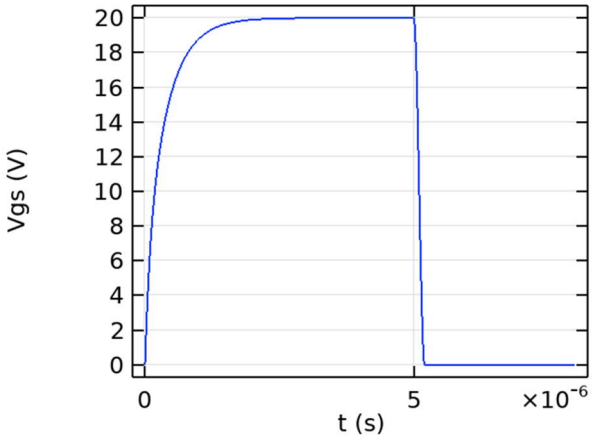

Figure 10 Chronogram of the voltage gate applied.

Overall, these shapes are fully consistent with experimental results obtained [11] and therefore validate the correct setting of the semiconductor properties of SiC.

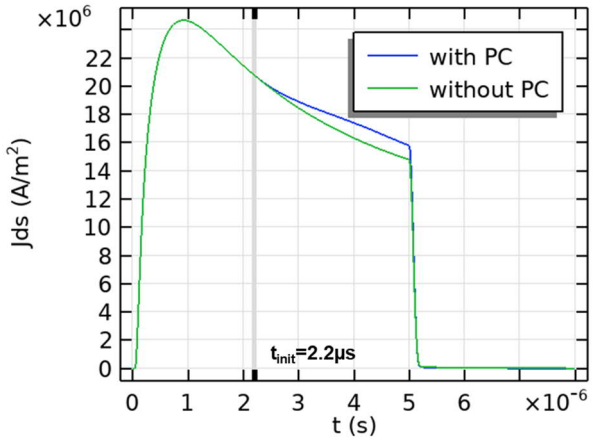

Figure 11 Chronogram of the resulting drain current density.

We now observe the effect of the phase change, which starts around 2.2µs. From this moment, as we explained in paragraph 2, the phase change induces significant energy absorption. Compared to a situation where the phase change is not considered, this attenuates the temperature dynamics in the SiC (figure 13), whose sensitivity will be all the greater as the region considered is close to the Al layer. Under these conditions, and due to the decrease in temperature of the SiC channel's mobility, an increase in current density is clearly observed but moderately because the main active region of SiC (JFET zone) is far from the fusion zone of the aluminum source electrode.

To check more precisely the internal thermal behavior of the transistor, we selected 3 points of interest judiciously placed for the measurement, as indicated in figure 12.

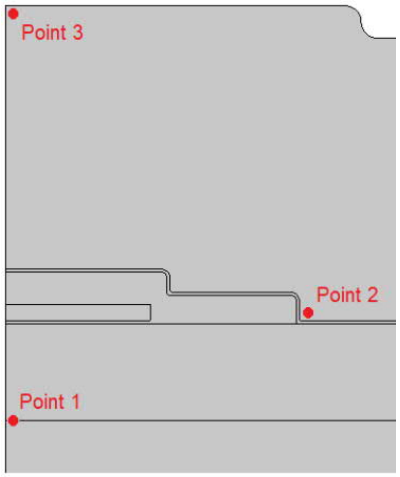

Figure 12 Points of interest for measurement.

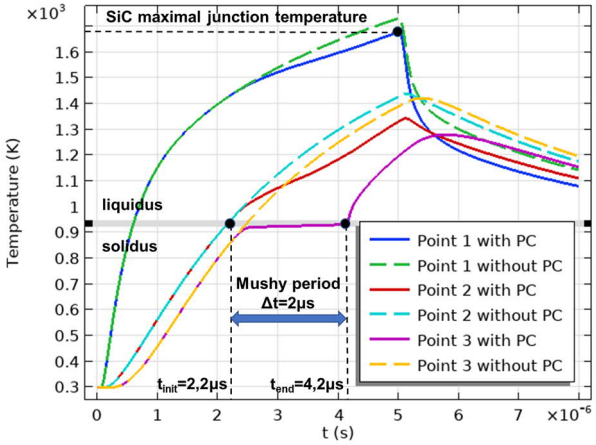

Figure 13 Chronograms of temperature with and without phase change at points 1, 2, and 3.

The temperature chronograms at the three measurement points are shown in figure 13 for the two situations with and without phase change. This figure allows us now to accurately extract the fusion start time $t_{init} = 2.2\mu s$ as well as the fusion end time $t_{end} = 4.2\mu s$. Between these two instants, the aluminum gradually liquefies (mushy period) and absorbs much energy. Knowing t_{init} is very important for the final user of the component because the chip will have to be protected by electronics to detect the short-circuit fault. The detection time must be less than t_{init} to avoid any memory effect and metallurgical aging of the chip so that it can accept several short-circuit cycles during its life. It is also verified in this figure that the maximum junction temperature does not exceed the runaway temperature (1400 K) by thermal generation specific to SiC under a polarization of $V_{DS} = 600V$ [15].

Figure 14 shows that the phase change at point 2, corresponding to the fusion beginning, is very fast. This small area of aluminum to the right of the gate is in direct contact with the very thin titanium bonding layer of the contact area of the source electrode. Heat spreads very quickly. On the other hand, at point 3, it is checked that the total melting of the aluminum layer, which represents a non-negligible volume, requires a delay $\Delta t = 4\mu s$. In the end, the phase change shows a 60K temperature attenuation at point 1 and a 100K at point 2. Therefore, the aluminum layer's heat sink property significantly reduces thermal stress and indirectly makes the chip more robust by limiting the temperature dynamics it has to undergo in extreme short-circuit conditions.

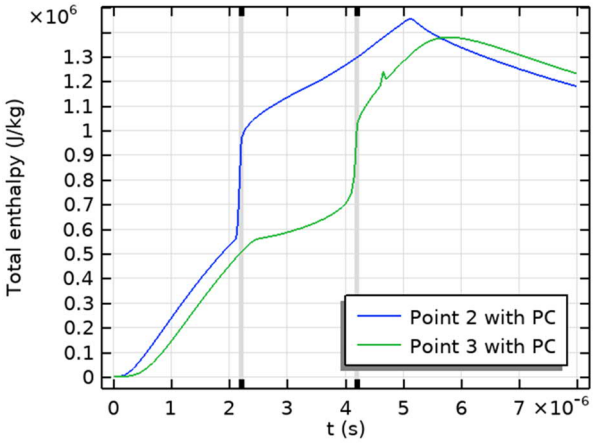

Figure 14 Chronograms of the enthalpy at points 2 and 3.

The phase change dynamics are also verified on the evolution of the heat capacity at points 2 and 3, as shown in Figure 15.

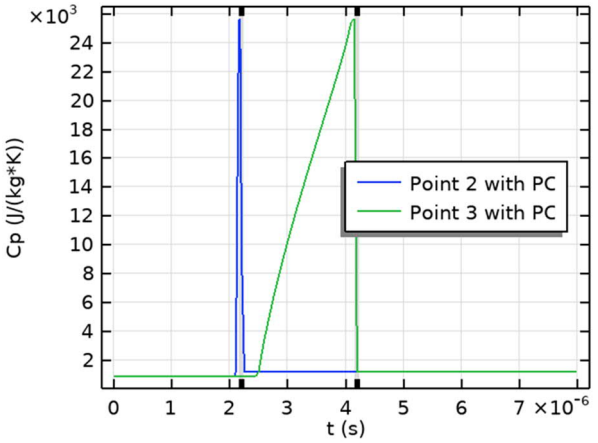

Figure 15 Chronograms of the heat capacity at points 2 and 3.

Figures 16 and 17 make it possible to illustrate more generally the propagation of the heat front in the transistor and that of the melting front in the metallic source electrode. These maps clearly indicate that the main heat zone inside the SiC corresponds well to that of point 1. This is the depletion zone (JFET zone) where the electric field and the current density are maximum, which induces maximum losses. It is also checked that points 2 and 3 make it possible to locate the zones of the start and end of melting of the source electrode.

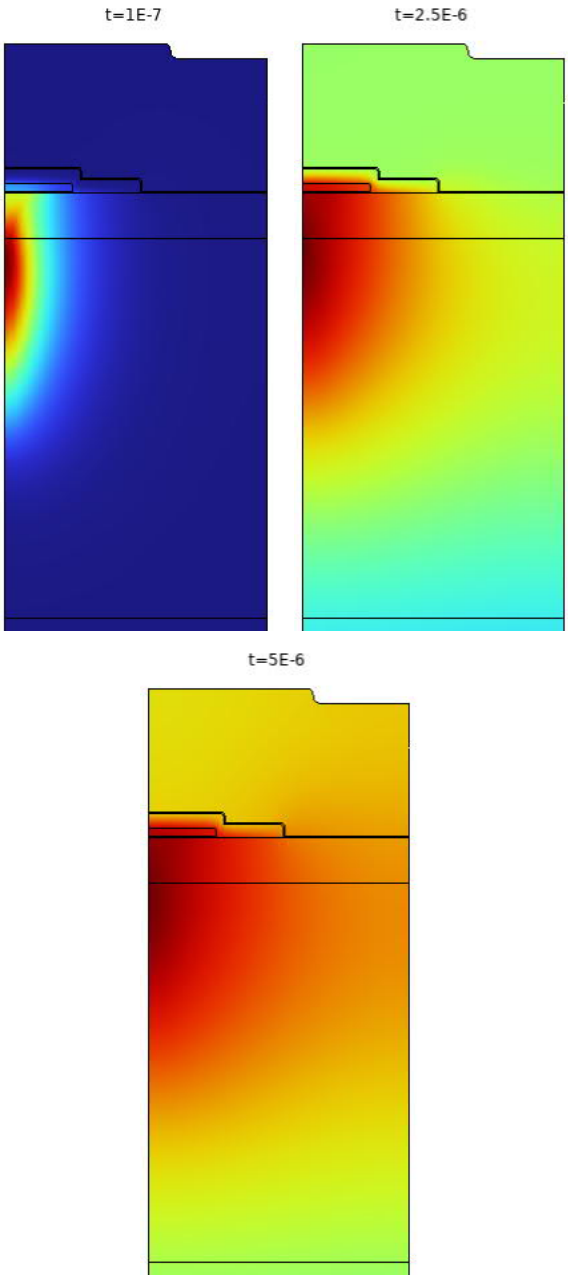

Figure 16 Temperature maps for three interesting times and dynamic visualization of the heat front.

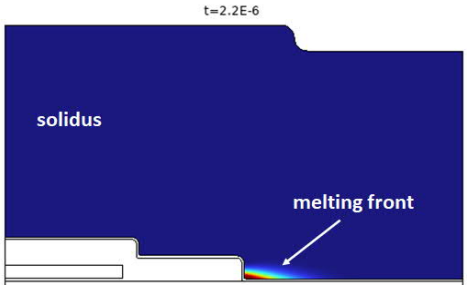

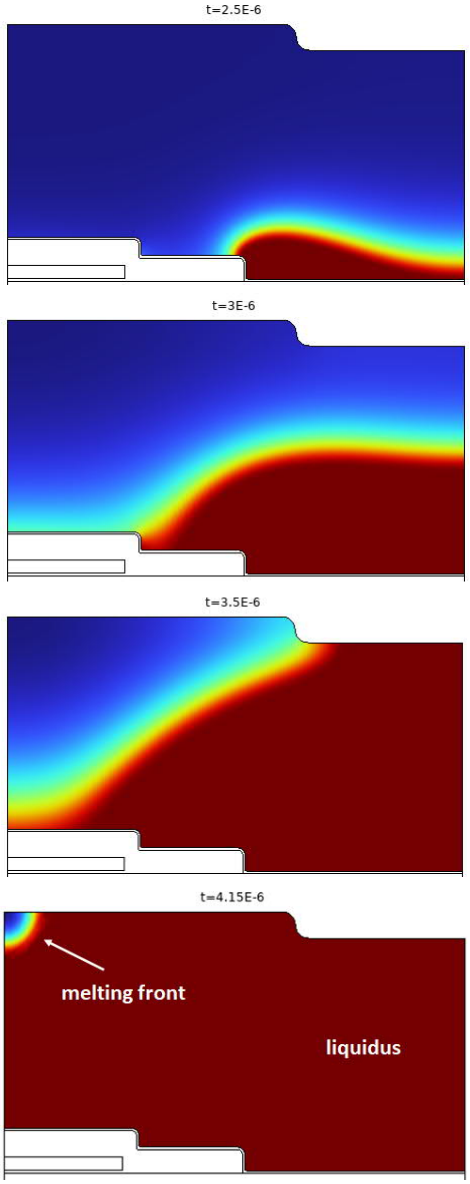

Figure 17 Maps of the phase change parameter α and dynamic visualization of the melting front.

5. Conclusion

For the first time, we have presented and developed a numerical model to fully simulate in 2D the dynamic electrothermal Al-source phase-change behavior of a SiC power transistor in short-circuit regime. The geometric precision of this model provides significant added values compared to existing 1D models. This model, therefore, constitutes a very important tool for phenomenological and technological understanding.

From the point of view of power converter users, the results obtained make it possible to very clearly identify the start $t_{init} = 2.2\mu s$ and end $t_{end} = 4.2\mu s$ melting times of source electrode. Those information are

essential, particularly for adjusting the maximum protection delay time of the device gate driver in the event of a short-circuit. Given that in practice, the initial temperature of the transistor can be well above 300K, it is necessary to take into account a safety margin. For long-life applications such as rail or solar, the triggering time can therefore be set below 1.5µs to avoid any risk of degradation on repeated short-circuit cycles.

For users too, these results show that, under a transistor bias at $V_{DS} = 600V$ and an initial temperature of 300K, the junction temperature remains below 1400 K before $t_{init} = 2.2\mu s$, thus avoiding any risk of avalanche. However, these results may change if the initial thermal conditions of the chip are modified.

Finally, from the component designer's point of view, this approach makes it possible to better understand the transistor's internal electrothermal phenomena, locate the areas of maximum stress and, therefore, correct the chip's design to make it more robust. For example, one can increase the thickness of the source electrode to increase the thermal inertia and to better spread out the total melting time. Other metal alloys can also be used to adapt their thermal conductivity or melting temperature.

Acknowledgments

Many thanks to Dr. Mustafa Shqair, a post-doctoral fellow at Lab. Laplace, for his help in the scientific presentation of the text of this article and for his contribution to the continuation of the work described in this article.

References

1. Adan, A. O. et al, "The Current Status and Trends of 1,200-V Commercial Silicon-Carbide MOSFETs: Deep Physical Analysis of Power Transistors from a Designer's Perspective," IEEE Power Electronics Magazine, Vol. 6, No. 2, pp. 36–47, 2019.
2. Robles, E. et al, "The role of power device technology in the electric vehicle powertrain," International Journal of Energy Research, Vol. 46, No. 15 (December 2022), pp. 22222-22265.
3. Castellazzi, A. et al, "Transient out-of-SOA robustness of SiC power MOSFETs," 2017 IEEE International Reliability Physics Symposium (IRPS), pp. 2A-3.1-2A-3.8.
4. Boige, F. et al, "Investigation on damaged planar-oxide of 1200V SiC power MOSFETs in non-destructive short-circuit operation," Microelectronics Reliability, Vol. 76–77, 2017, pp. 500-506.
5. Richardeau, F. et al, "Circuit-type modelling of SiC power Mosfet in short-circuit operation including selective fail-to-open and fail-to-short modes competition," Microelectronics Reliability, Vol. 100–101, 2019.
6. Pascal, Y. et al, "Thermal simulations of SiC MOSFETs under short-circuit conditions: influence of various simulation parameters," 2019 IEEE International Workshop on Integrated Power Packaging (IWIPP), Toulouse, France, 2019, pp. 137-142.
7. Loche-Moinet, F. et al, "Apparent heat capacity model of the SiC MOSFET's Aluminium top surface for short-circuits simulations," 2022 23rd International Conference on Thermal, Mechanical and Multiphysics Simulation and Experiments in Microelectronics and Microsystems (EuroSimE), St Julian, Malta, 2022, pp. 1-6.
8. Nguyen, T.A. et al, "Investigation on the junction temperature of planar power 4H-SiC MOSFET under short circuit operation ", Microelectronics Reliability, Vol. 138, 2022.
9. Shoji, T. et al, "Dependence of Short-Circuit Withstand Capability of SiC MOSFETs on Short-Circuit Failure Time ", in IEEE Transactions on Power Electronics, vol. 36, no. 10, pp. 11739-11747, Oct. 2021.
10. Romano, G. et al, "A Comprehensive Study of Short-Circuit Ruggedness of Silicon Carbide Power MOSFETs ", in IEEE Journal of Emerging and Selected Topics in Power Electronics, vol. 4, no. 3, pp. 978-987, Sept. 2016.
11. Jouha, W. et al, "Gate-damage safe failure-mode deep analysis under short-circuit operation of 1.2kV and 1.7kV power SiC MOSFET using dedicated gate-source / drain-source voltage depolarization and damage-mode optical imaging ", 2022 IEEE Workshop on Wide Bandgap Power Devices and Applications in Europe (WiPDA Europe), Coventry, United Kingdom, 2022, pp. 1-6.
12. Comsol documentation, https://www.comsol.fr/
13. Mohamad Muhieddine, Edouard Canot, Ramiro March, Various Approaches for Solving Problems in Heat Conduction with Phase Change, International Journal on Finite Volumes, Institut de Mathématiques de Marseille, AMU, 2009, pp.19. hal-01120384v2.
14. Faruk Civan, C.M. Sliepcevich, Limitation in the Apparent Heat Capacity Formulation for Heat Transfer with Phase Change, Proc. Okla. Acad. Sci. 67:83-88 (1987).
15. Cyril Buttay, Christophe Raynaud, Hervé Morel, Gabriel Civrac, Marie-Laure Locatelli, and al., Thermal stability of silicon-carbide power diodes, IEEE Transactions on Electron Devices, 2012, 59 (3), pp.761-769, 10.1109/TED.2011.2181390, hal-00672440.